Image Cover Sheet

CLASSIFICATION	SYSTEM NUMBER
UNCLASSIFIED	509382

TITLE

MULTIPLE-SCATTERING EFFECT ON OZONE RETRIEVAL FROM SPACE-BASED DIFFERENTIAL ABSORPTION LIDAR MEASUREMENTS

System Number:

Patron Number:

Requester:

Notes:

DSIS Use only:

Deliver to:

Multiple-scattering effect on ozone retrieval from space-based differential absorption lidar measurements

Shiv R. Pal and Luc R. Bissonnette

Single-scattering and multiple-scattering lidar signals are calculated for a spaceborne differential absorption lidar system for global ozone measurements at the on and off wavelength pair at 305 and 315 nm. The effect of multiple scattering is found to be negligible on stratospheric and tropospheric ozone retrieval under background stratospheric aerosol. Under low-visibility conditions in the planetary boundary layer the presence of multiple scattering causes an overestimation in maritime aerosol and an underestimation in urban as well as in rural aerosol. This effect is also examined in three cirrus models. The multiple scattering does not permit accurate ozone retrieval within cirrus; however, below it the solution recovers somewhat with generally an underestimation depending on the type and density of cirrus. The effect of aerosol and Rayleigh extinction on the ozone retrieval is also discussed.

OCIS code: 290.0290.

1. Introduction

After the success of the Lidar in Space Technology Experiment (LITE) mission onboard the Space Shuttle Discovery in September 1994,[1] several spaceborne lidar applications have been conceived and programs for global coverage with lidar have been proposed. The feasibility studies are underway on several programs, such as the atmospheric lidar for cloud detection under the European Space Agency and the Ozone Research with Advanced Cooperative Lidar Experiment (ORACLE) for global ozone under a collaboration between the Canadian Space Agency and the NASA Langley Research Center. A careful feasibility study of a spaceborne system is more critical than that of a ground-based system, owing to inaccessibility of the system for introducing changes. Therefore for an optimum space-qualified reliable system its feasibility study requires a critical review of factors that affect the lidar system design parameters. Once the feasibility of the lidar components is initially worked out, performance calculations require a realistic atmospheric model profile to determine accuracies of measurements. If the accuracy is lower than required, the lidar parameters are altered and an iteration finally determines the concept of the final lidar system. In the case of a spaceborne lidar system large scattering distances and resulting large scattering volumes are involved. Therefore it becomes necessary to examine the effect of multiple scattering (MS) on the lidar performance and on the required accuracy. Here we discuss the effect of MS on the accuracy of ozone measurement with a spaceborne ozone differential absorption lidar (DIAL) system.

In ozone DIAL operation two closely spaced wavelengths, λ_{on} (highly absorbed by ozone) and λ_{off} (reference wavelength not absorbed by ozone), are utilized to give high differential absorption and negligible differential scattering at the two wavelengths. The ozone profile is derived from the slope of the ratio of backscatter signals, $P_{on}(z)$ and $P_{off}(z)$. At first glance it therefore appears reasonable to anticipate that a single-scattering (SS) consideration would suffice to estimate ozone concentration and that the effect of MS, if any, at the two wavelengths would cancel out. This, however, is not the situation, as is shown in the following.

In space DIAL application, as the laser pulse traverses into increasing tropospheric and highly variable planetary boundary-layer (PBL) aerosol, the

S. R. Pal is with the Centre for Research in Earth and Space Technology, 4850 Keele Street, North York, Ontario M3J 1K3, Canada. L. R. Bissonnette is with the Defense Research Establishment Valcartier, 2459 Pie XI Blvd. North, Val-Belair, Quebec, G3J 1X5, Canada.

Received 24 December 1997; revised manuscript received 4 May 1998.

0003-6935/98/276500-11$15.00/0

MS effect is expected to increase with distance. Also, owing to large distances involved, the lidar footprint would include large scattering volumes resulting in a large number of available photon paths. Here we present the study of MS for a typical DIAL system as conceived in the ORACLE program but with differing lidar system parameters. In this study clear atmospheric conditions in the troposphere are considered with high visibility (HV) and low visibility (LV) in the PBL. Since cirrus clouds are globally prevalent, we also include a study of the feasibility and accuracy of ozone measurements by means of cirrus.

The influence of MS on trace-gas concentration retrieved by DIAL techniques has been simulated by Ben-David[2] but in transmission only and with plane-parallel wave geometry. MS contributions by cirrus clouds in spaceborne lidar measurements have also been calculated by Flesia and Starkov.[3] Both studies demonstrate potentially serious effects.

Table 1. Space DIAL System Parameters

Parameter	Value
λ_{on}, λ_{off}	305, 315 nm
Lidar altitude	300 km
Laser energy	480 mJ
Beam diameter	700 mm
Beam divergence	0.1 mrad
Pulse length	30 ns
Telescope diameter	1 m
Receiver bandwidth	1 nm
Receiver field of view	0.5 mrad

2. Simulation

A. System Parameters

The DIAL system parameters and satellite altitude in the ORACLE program are currently being finalized. Therefore the set of lidar parameters adopted for this study are for a typical DIAL system, and its general conclusions are applicable for a typical spaceborne DIAL system. The lidar parameters are given in Table 1.

B. Ozone Differential Absorption Lidar Equations

The standard lidar equations for on and off wavelengths with parameters subscripted as on and off, respectively, are given in

$$P_{on}(z) = P_{ton}\eta_{on}\frac{A}{z^2}\frac{ct}{2}\beta_{on}(z)\exp\left[-2\int_0^z \sigma_{on}(z')dz\right],$$

$$P_{off}(z) = P_{toff}\eta_{off}\frac{A}{z^2}\frac{ct}{2}\beta_{off}(z)\exp\left[-2\int_0^z \sigma_{off}(z')dz\right],$$

where P_t is the transmitted laser power, η is the system efficiency, A is the effective receiver area, $ct/2$ is the laser pulse length, and z is the range of scattering. The atmospheric parameters β and σ represent the backscatter and extinction coefficients, respectively. The derivatives of the logarithmic ratios provide the DIAL equation for ozone number density, the $n_{O3}(z)$ profile, in terms of O_3 absorption cross sections Ω_{O3}, Rayleigh scattering cross sections Ω_R, Rayleigh number density $n_R(z)$, and aerosol (Mie) extinction coefficients $\sigma_M(z)$, given as

$$n_{O3}(z) = \frac{1}{2\Delta\Omega_{O3}}\left\{\frac{d}{dz}\ln\left[\frac{P_{off}(z)}{P_{on}(z)}\right]\right\} - \frac{1}{\Delta\Omega_{O3}}n_R(z)\Delta\Omega_R - \frac{1}{2\Delta\Omega_{O3}}\left\{\frac{d}{dz}\ln\left[\frac{\beta_{off}(z)}{\beta_{on}(z)}\right]\right\} - \frac{1}{\Delta\Omega_{O3}}\Delta\sigma_m(z) \quad (1)$$

or

$$n_{O3}(z) = T_P - T_R - T_\beta - T_\sigma, \quad (2)$$

where

$$\Delta\Omega_{O3} = \Omega_{O3,on} - \Omega_{O3,off},$$

$$\Delta\Omega_R = \Omega_{R,on} - \Omega_{R,off},$$

$$\Delta\sigma_M(z) = \sigma_{M,on}(z) - \sigma_{M,off}(z).$$

The main contribution to ozone number density is from the term T_P. The subtractive terms provide corrections to ozone number density caused by differential scattering owing to Rayleigh extinction (T_R), aerosol plus Rayleigh backscatter (T_β), and Mie extinction (T_σ). In this simulation it was found that it is important to apply corrections owing to the three terms. This requires that in the same experiment the information on Rayleigh and Mie atmospheres be derived simultaneously from $P_{on}(z)$ and $P_{off}(z)$ (see Ref. 4) or from other ancillary lidar wavelengths if available (for example, as proposed by Kovalev and Bristow[5]).

The lidar returns $P_{on}(z)$ and $P_{off}(z)$ for SS and MS were calculated for the assumed lidar system with pulse transmission in a model atmosphere, and corresponding ozone number densities were calculated. The effect of the terms T_R, T_β, and T_σ on the accuracy of ozone concentration was also studied.

C. Model Atmosphere

Although the lidar range is 300 km, the model atmosphere is extended to only 100 km. The total molecular and ozone density profiles are given at discrete altitudes with a resolution of 1 km below 25 km and a gradually degraded resolution from 25 to 100 km. The small difference between the wavelengths 305

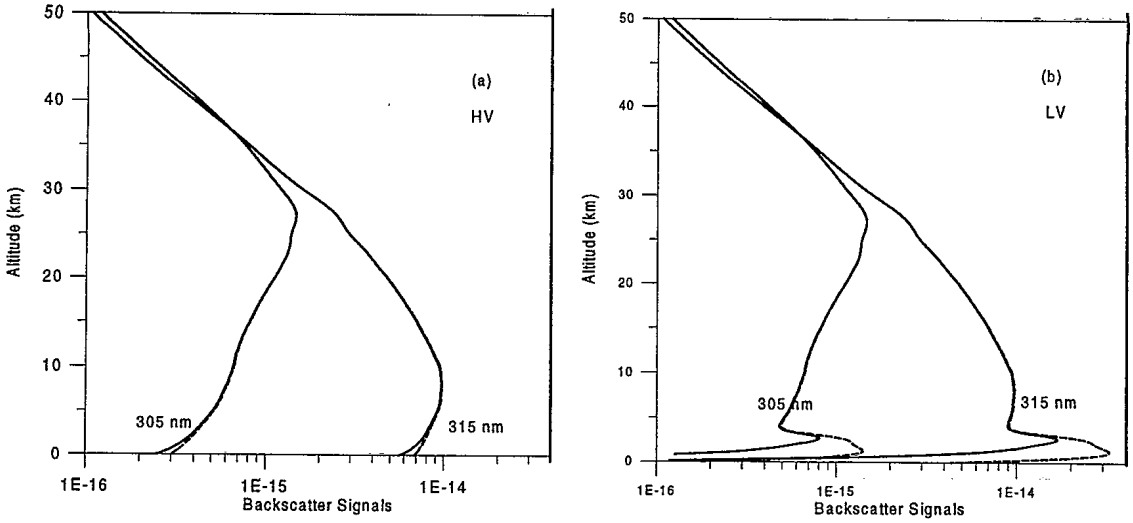

Fig. 1. (a) $P_{on}(z)$ and $P_{off}(z)$ for SS (solid curves) and for MS (dashed curves) in (a) HV and (b) LV.

and 315 nm requires highly accurate absorption coefficients at the two wavelengths.

We also specify on the same grid an aerosol profile. At altitudes higher than 15 km we use the scattering phase function defined by the LOWTRAN stratospheric aerosol model. For the troposphere between 3 and 15 km the phase function is calculated from the LOWTRAN 75% relative humidity maritime-continental aerosol model. The remaining 3 km define the PBL. Two cases are considered: (1) a HV case with a ground-level visible range of 25 km modeled by the LOWTRAN 75% relative humidity maritime-continental aerosol and (2) a LV case with a ground-level visible range of 5 km modeled by the LOWTRAN 99% relative humidity maritime-oceanic aerosol. There is no specific reason to choose maritime-continental aerosol or maritime-oceanic aerosol for different visibilities. However, a maritime component was chosen for most calculations because of the fact that a large fraction of the satellite ozone coverage would relate to ocean surface. The calculations for other types of aerosol were also performed, and the results are briefly discussed here.

In addition, we consider three models of cirrus clouds: cold cirrus (CC), warm cirrus (WC), and cirrus uncinus (CU) adopted from Heymsfield[6] and Heymsfield and Platt.[7] We calculated the scattering phase functions for these clouds assuming spherical ice particles. Their hexagonal size distributions in terms of crystal length were translated into spheres of equivalent surface area. The spheres of equivalent surface area were adopted because in a separate calculation it was found that the ice spheres of equivalent surface area gave better consistency of scattering parameters than ice spheres of equivalent volumes. For Mie calculations choosing equivalent spheres is a reasonable approximation for the small-angle forward scatterings but not realistic for backscatter. However, this is acceptable for the purpose of the present simulations since the objective is to investigate where and how multiple scattering may influence the retrieval of ozone concentrations; the exact magnitude of the effect is not our primary goal. In this study cirrus clouds are modeled by a Gaussian layer centered at an altitude of 12 km. The effect of the change of optical depth and cloud geometrical thickness is also examined. All input profiles are interpolated on a uniform grid of 100-m steps, and the lidar calculations are performed at a resolution of 100 m.

D. Multiple-Scattering Model

We use the analytical model of Bissonnette[8] modified by the equivalence theorem of Katsev *et al.*,[9] which implies that the recorded multiple-scattered lidar returns from a given medium are the same as would be obtained from a fictitious medium that has twice the extinction coefficient but the same angular-scattering properties as the true medium in the forward direction, along with zero extinction in the backward direction. The model is further extended to take into account the forward geometrical-optics scatterings.

The simulations include both Rayleigh and aerosol scatterings. One basic approximation of the model is that it assumes a single backscattering[10] at an angle close to 180° preceded and followed by multiple small-angle forward scatterings in the forward and backward propagation paths, respectively. This means that the range resolution is conserved. Over the large distances involved in space measurements, the approximation is valid if the receiver footprint is smaller than the scattering mean free path. In cirrus clouds space-based LITE measurements[11] have confirmed that there are no significant pulse-stretching effects caused by multiple scattering at fields of view of the order of 1 mrad. For the tropospheric aerosols used here, the ground-level-scattering mean free path in the worst case of LV is 300 m compared with the 150-m receiver footprint. Therefore the approximation is valid and the model applicable to the assumed problem.

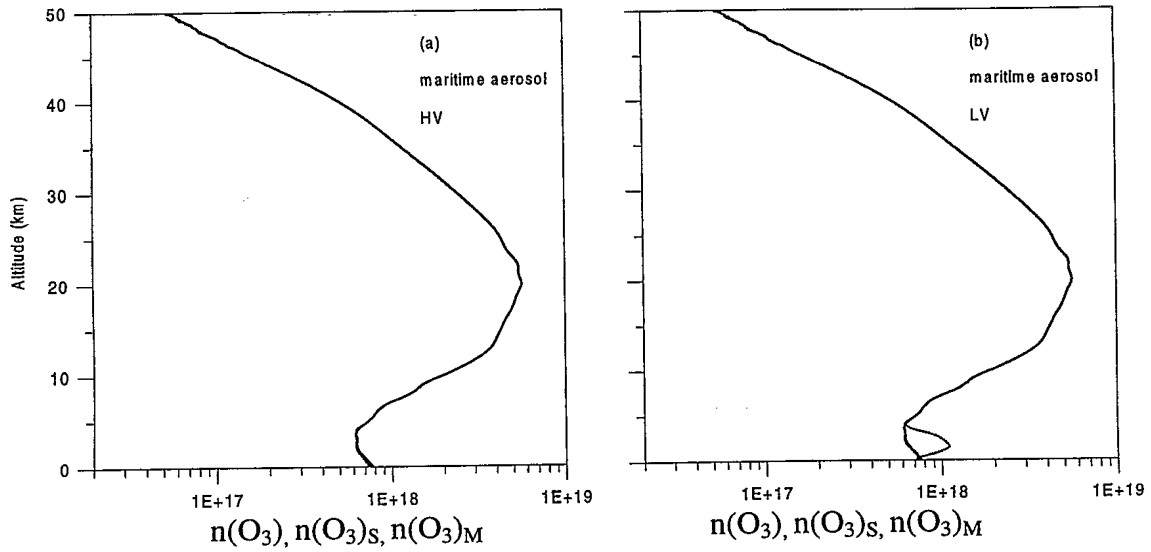

Fig. 2. Model O_3 profile (dashed curve), retrieved SS (solid curve), and MS (dotted curve) for the (a) HV and (b) LV boundary layer for maritime aerosol.

3. Results

A. Differential Absorption Lidar Simulation

In the present DIAL simulation the lidar backscatter signals $P_{on}(z)$ and $P_{off}(z)$ for SS and MS are calculated for the composite atmosphere described above. These signals are then utilized to calculate ozone profiles corresponding to SS and MS. The SS profiles at λ_{on} and λ_{off} for maritime aerosol are shown in Fig. 1(a) for HV and in Fig. 1(b) for LV.

$P_{on}(z)$ and $P_{off}(z)$, which represent mainly the Rayleigh scattering, from the satellite to approximately 45-km altitude, run parallel to each other. Below this altitude the stratospheric ozone starts to show differential absorption at λ_{on} and λ_{off}. The continued ozone profile in the stratosphere to as low as the ground level creates a large reduction in $P_{on}(z)$. $P_{on}(z)$ and $P_{off}(z)$ for MS (dotted curves) show an increase in the PBL. In LV the increase in backscatter signals owing to MS is much larger than in HV.

Figures 2(a) and 2(b) present ozone number density profiles, $n(O_3)_S$ (solid curve) and $n(O_3)_M$ (dotted curve) for SS and MS, respectively, as retrieved from the backscatter returns in Figs. 1(a) and 1(b). In this retrieval the correction terms T_R, T_β, and T_σ were also included. A third profile shown in Fig. 2 by the dashed curve is the input model ozone profile. The three curves are coincident for most of the profile and therefore are indistinguishable. As can be seen in the HV as well as in the LV PBL, $n(O_3)_S$ coincides with $n(O_3)$ right up to the ground level, indicating that the retrieval equation and the estimation of the correction terms is very accurate. $n(O_3)_M$ in HV does not seem to depart much from the model, whereas in LV it shows considerable departure within the PBL.

A change in character of aerosol from maritime as above to urban or rural introduces a change in scattering phase function sufficient to alter the effect of MS on ozone retrieval in the PBL; however, for SS the three types of aerosol give nearly the same result. This is shown in Fig. 3, where the effect of MS is to give an underestimation of ozone retrieval (dotted curve). To draw this comparison, we present the LV case here because an appreciable MS-induced change in retrieved ozone values by means of a change in the aerosol occurs in LV only.

To see the proportion of the overestimation or underestimation of ozone caused by the MS contribution with respect to ozone retrieval from SS, we show the ratio $n(O_3)_M/n(O_3)_S$ in Fig. 4(a) for maritime HV, in Fig. 4(b) for maritime LV, and in Fig. 4(c) for urban and rural aerosol in LV. Although the MS starts to contribute as the pulse enters the troposphere, its effect becomes obvious only from an approximately 4-km altitude. In maritime HV the effect of MS is to show a gradual reduction in ozone by approximately 5% near the ground level. In maritime LV the effect is an overestimation of ozone reaching a maximum at approximately 68% in the middle of the PBL and then a decrease with values coming close to and below the SS values. When the maritime LV in Fig. 4(b) is compared with the urban and rural LV in Fig. 4(c), one finds that the MS in urban and rural aerosol causes an underestimation of ozone retrieval similar to the HV case of maritime in Fig. 4(a). The difference, however, is that the urban aerosol causes an underestimation at the ground level of approximately 30% and the rural aerosol causes one of approximately 13%, as compared with the 5% in HV maritime aerosol.

B. Effect of Correction Terms

The calculations presented in the above figures are with the correction terms T_R, T_β, and T_σ [shown in Eq. (2)] included in Eq. (1). Since the model atmosphere provides the input for calculation of the three terms in this simulation, a realistic estimate of the

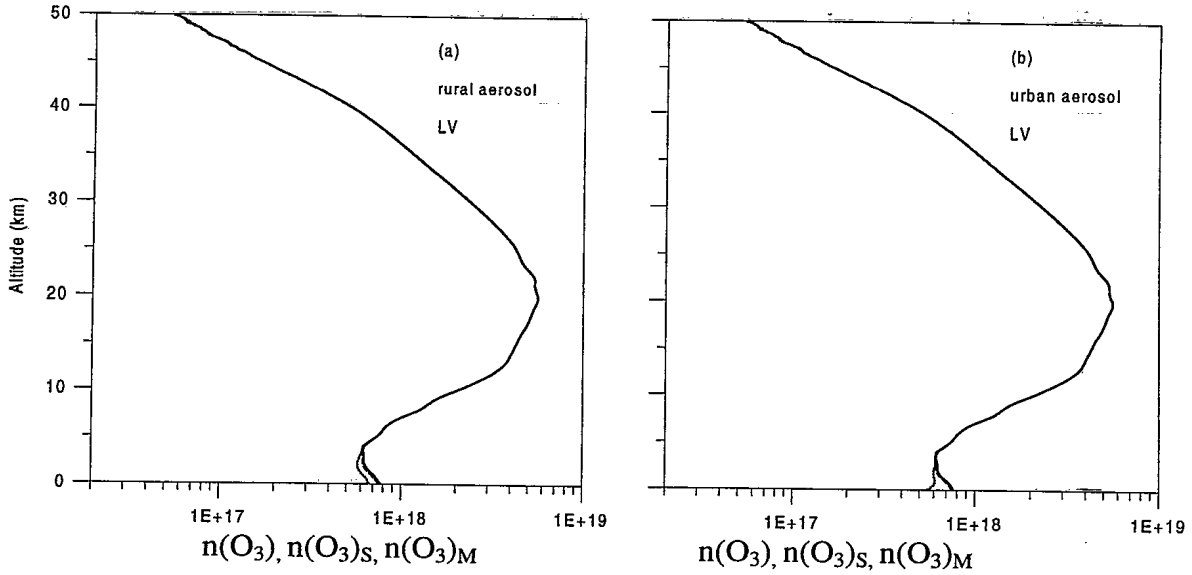

Fig. 3. Model O_3 profile (dashed curve), retrieved SS (solid curve), and MS (dotted curve) for (a) rural aerosol and (b) urban aerosol in the LV boundary layer.

correction terms was possible. In real application of spaceborne DIAL this information is not easily available. We show the effect of these three terms in the following by taking the example of HV and LV maritime aerosol.

Figure 5 presents four ozone profiles corresponding to the four terms in Eq. (2) for HV [Fig. 5(a)] and for LV [Fig. 5(b)]. $n(O_3)_S$ is the uncorrected SS ozone profile that corresponds to the first term T_P. The relative contributions of the so-called correction terms are labeled T_R, T_β, and T_σ. Since these terms vary over several orders of magnitude below the main ozone profile, the scale on the x axis contains several more decades of values as compared with Figs. 2 and 3.

The subtractive contribution of the three terms to the ozone profile is negligibly small for most of the troposphere and the stratosphere, with the T_β contribution higher than the T_σ contribution and the one caused by T_R higher than the other two. However, the contribution becomes substantial in the lower troposphere and in the PBL, especially with LV in it enhancing the contribution of the backscatter term T_β. Note that the peak in uncorrected $n(O_3)_S$ in the LV case [Fig. 5(b)] corresponds to the peak in T_β.

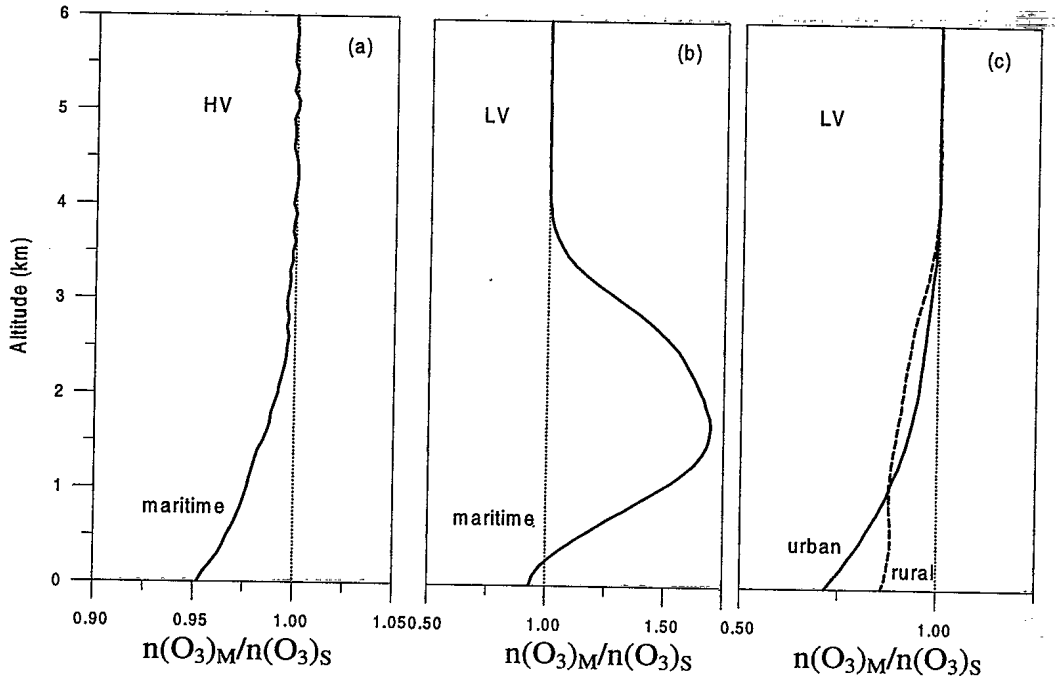

Fig. 4. Ratio of MS to SS ozone profiles for (a) HV maritime, (b) LV maritime, and (c) LV rural and urban aerosol.

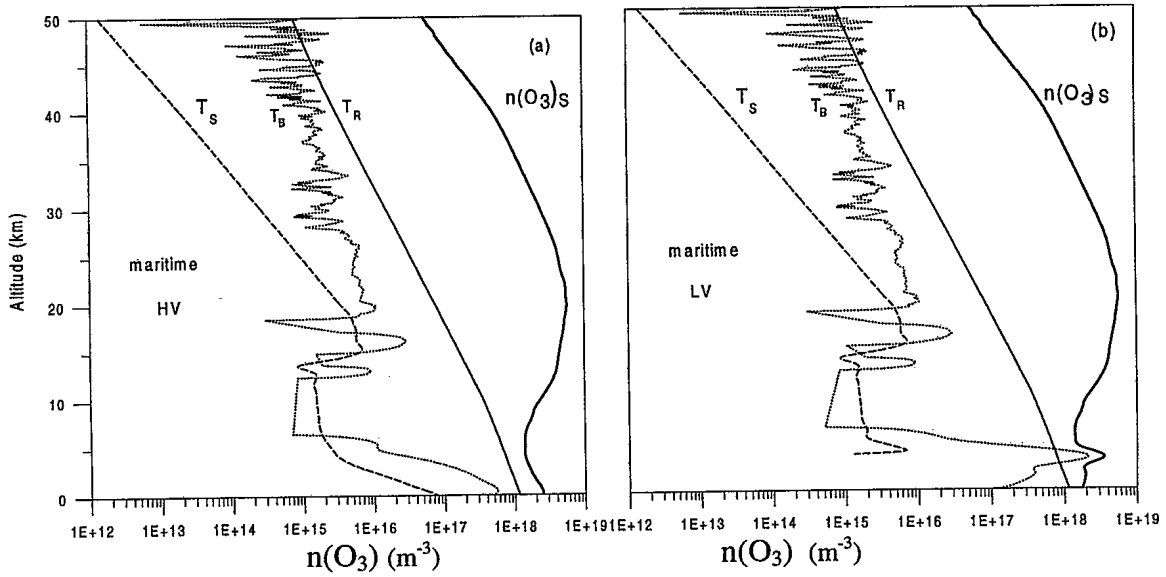

Fig. 5. Uncorrected SS ozone profile $n(O_3)_S(T_P)$ and the correction terms T_R, T_β, and T_σ for maritime aerosol in (a) HV and (b) LV.

Since all correction terms are subtractive and are below the uncorrected ozone profile, a retrieved solution without correcting for the three terms would give an overestimated ozone profile.

When the aerosol loading is higher in the troposphere or even in the stratosphere after a volcanic eruption, the aerosol correction terms become measurable, especially T_β, to contribute to errors in ozone measurements in the DIAL. The effect of T_β and T_σ on the accuracy of stratospheric ozone retrieval by the DIAL in the presence of Pinatubo aerosol was discussed in detail by Steinbrecht and Carswell.[4] The stratospheric volcanic aerosol usually declines after an eruption, reaching background levels that permit ozone measurements without rigorous corrections owing to these terms. However, because the aerosol in the troposphere and in the PBL in particular is highly variable on a global basis, a space-based DIAL is required to measure aerosol scattering simultaneously with ozone measurements.

To see the effect of neglecting the correction terms on the ozone profiles for SS and MS in HV's and LV's for a marine environment, we plotted the model ozone profile along with the estimated SS and MS ozone profiles in Fig. 6. The overestimation of ozone above the model profile (dashed curve) is seen to increase for SS and MS from the stratosphere toward the ground level. In HV the overestimation for SS and MS is practically the same. In the case of LV in Fig. 6(b) both SS and MS exhibit a peak at the top of the

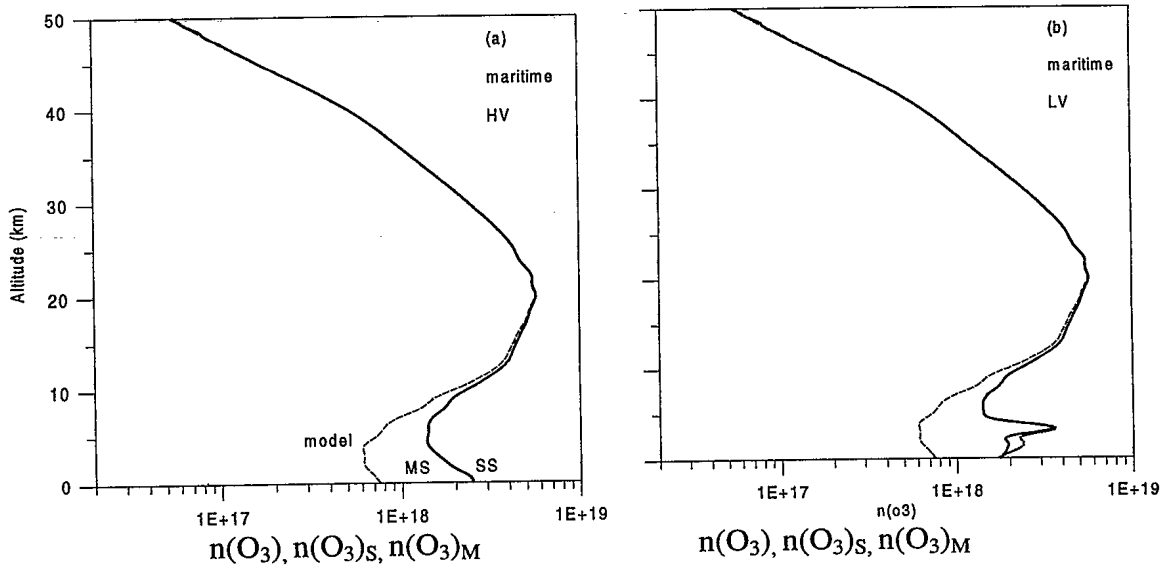

Fig. 6. Model ozone profile (dashed curve), SS ozone profile (solid curve), and MS ozone profile (dotted curve) for (a) HV and (b) LV maritime aerosol. The SS and MS ozone profiles are without correction terms applied.

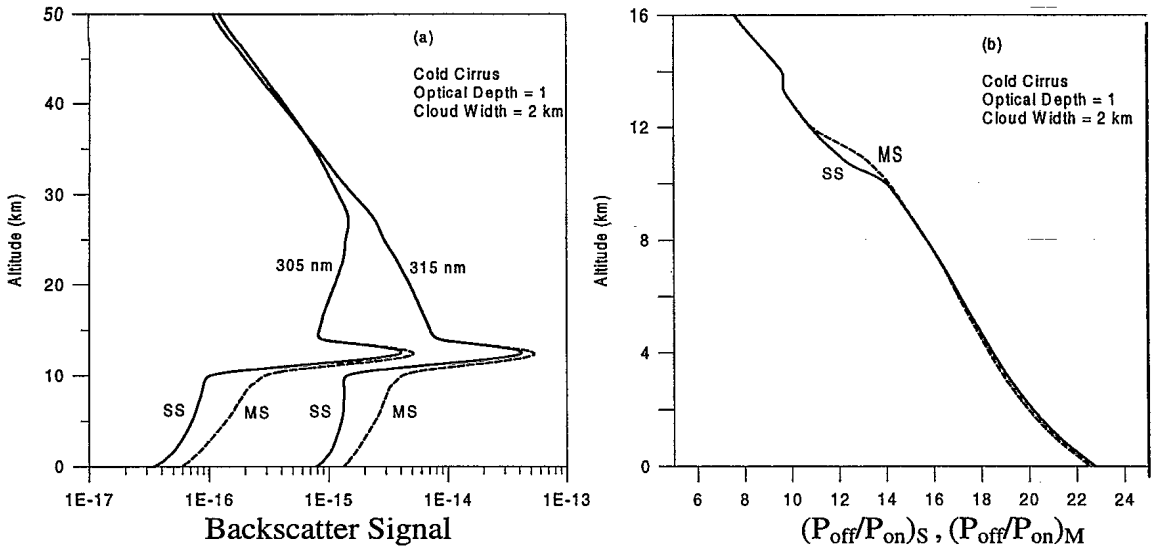

Fig. 7. (a) Backscatter signals at the two DIAL wavelengths for SS (solid curve) and MS (dashed curve) in the presence of CC peaked at 12 km with $\Delta z = 2$ km and $\tau = 1$. (b) Ratio of signals for off and on wavelengths for the same CC for SS (solid curve) and with MS included (dashed curve).

boundary layer, with MS showing even higher overestimation of ozone. This peak is the result of the nature of the DIAL analysis that uses the slope of the ratios of the measured signals [Eq. (1)]. The slope is determined along the signal profiles by use of a sliding window of a number of points. When there is a drastic change in this slope, owing to a transition in the backscatter coefficient caused by a change in aerosol layer, the slope method produces an excursion of ozone values. The aerosol model may be continuous in its extinction coefficient but discontinuous in aerosol type, causing a transition in the effective phase function and therefore in the backscatter coefficient. Thus the values around this excursion are not reliable and may not be realistic because in the natural atmosphere we expect continuity in both extinction and backscattering coefficients. However, when the dominant correction term T_β is available, which is also derived from the slopes of backscatter coefficients, such excursions are subtracted out and the ozone value becomes reasonably acceptable, as shown in Fig. 3, where the correction terms were accounted for.

C. Model Cirrus

The cirrus clouds generally confined below the tropopause level do not affect space DIAL application for stratospheric ozone. They, however, pose a serious problem for tropospheric ozone measurements in several ways. On one hand, the attenuation by a cirrus at the DIAL wavelengths would reduce strengths of backscatter signals, reducing the ozone retrieval accuracy; on the other hand, it would introduce a measurable effect of the correction terms T_β and T_σ, causing a further reduction in the ozone retrieval accuracy. These factors, when strong enough, may not permit ozone retrieval in the presence of cirrus. For global ozone retrieval this difficulty is further compounded by the fact that the cirrus are ubiquitous in nature, thus affecting global ozone retrieval in general. As shown in the following, the tenuous and subvisual cirrus may still permit decent ozone measurements below them.

One other source of error in DIAL ozone measurement is MS in cirrus similar to the effect of aerosol examined in Subsections 3.A and 3.B. For the study of MS in cirrus clouds and its effect on ozone retrieval, three types of cirrus, CC, WC, and CU, were considered. The cirrus are assumed to have a Gaussian profile with the peak centered at 12 km. We first used a geometric thickness of 2 km at $1/e$ points to see the effect on ozone retrieval and the effect of change in effective phase functions caused by the three types of cirrus. Then to see the effect of increased photon paths we doubled the geometric thickness to 4 km, keeping the same optical depth. The effect of increased optical depth was also examined. The backscatter signals from all these cirrus combinations were determined with cirrus profiles superimposed on the model atmosphere with HV maritime aerosol.

Figure 7(a) shows the backscatter signals at two DIAL wavelengths for a CC with a geometrical thickness of $\Delta z = 2$ km and an optical depth of $\tau = 1$. The signals on the top side of CC are similar to those in Fig. 1 (clear air), with the presence of cirrus showing a strong enhancement as the MS builds up (dashed curves).

The backscatter at MS shows a higher level than at SS, beginning in the cloud and persisting below it right up to the ground level. This is consistent with the Monte Carlo calculations of Flesia and Starkov.[3] The signal ratios $(P_{off}/P_{on})_S$, $(P_{off}/P_{on})_M$ in the presence of SS and MS, respectively, which directly take part in ozone calculations, are shown in Fig. 7(b). Both ratios exhibit a depression as the pulse enters

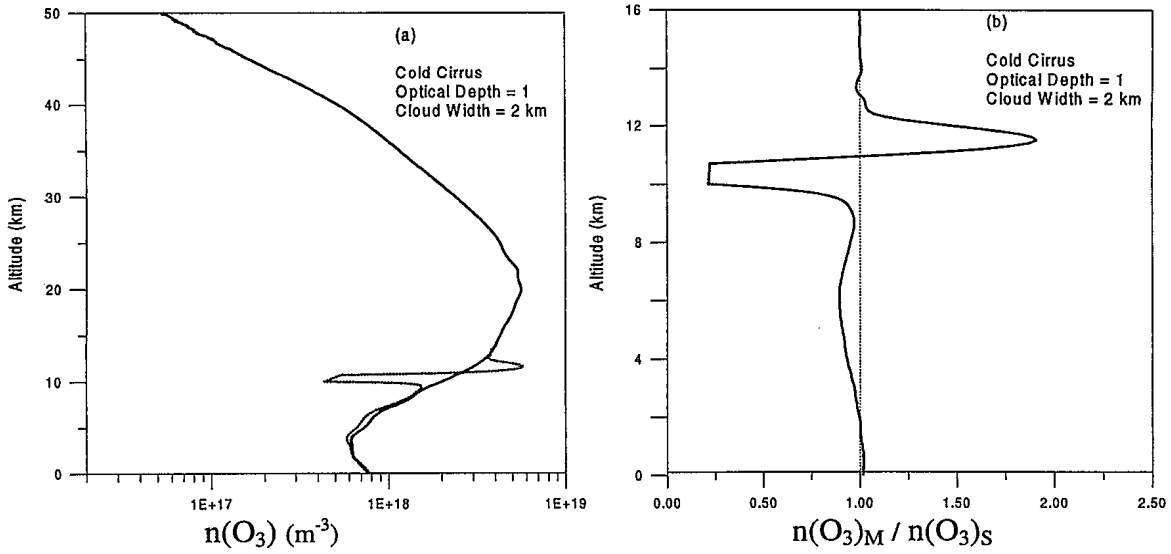

Fig. 8. (a) Model ozone profile (dashed curve), retrieved SS ozone profile (solid curve), and MS ozone profile (dotted curve) in the presence of CC peaked at 12 km with $\Delta z = 2$ km and $\tau = 1$. (b) Ratio of retrieved profiles with MS included and with SS only.

the cloud, with the ratio for MS starting to show a significant buildup in the middle of the cloud near the cloud peak. The merging of MS and SS curves at the bottom of the cloud makes it obvious that the MS effect on the ratio is insignificant as soon as the pulse exits the cloud. Calculations of Flesia and Starkov[3] show a steep and narrow peak of the multiple-to-single-scattering ratio just below the cloud layer caused by the temporal delay of the MS paths compared with the SS paths. This effect does not exist in our simulations since the analytical model neglects pulse stretching altogether. Incidentally, the peak shown by Flesia and Starkov[3] would probably be much less evident here because our Gaussian model cloud has a diffuse boundary compared with their binary cirrus layer.

For the data in Fig. 7 the ozone profiles $n(O_3)_S$ (solid curve) and $n(O_3)_M$ (dotted curve), with correction terms accounted for, are shown in Fig. 8(a). The original model ozone profile $n(O_3)$ is also plotted as the dashed curve that coincides with the $n(O_3)_S$ curve. When the extinction and backscatter values for the cirrus and the atmosphere are available, as in this model calculation, the ozone retrieval in the presence of cirrus is possible with considerable accuracy. However, the presence of MS causes a drastic change in the slope of the signal ratios to cause a fluctuation in retrieved ozone. The effect of MS is exhibited in the ratio of retrieved ozone for MS and SS in Fig. 8(b). The ratio of 1 represents the absence of the influence of MS.

The ozone ratio $n(O_3)_M/n(O_3)_S$ shows a large in-

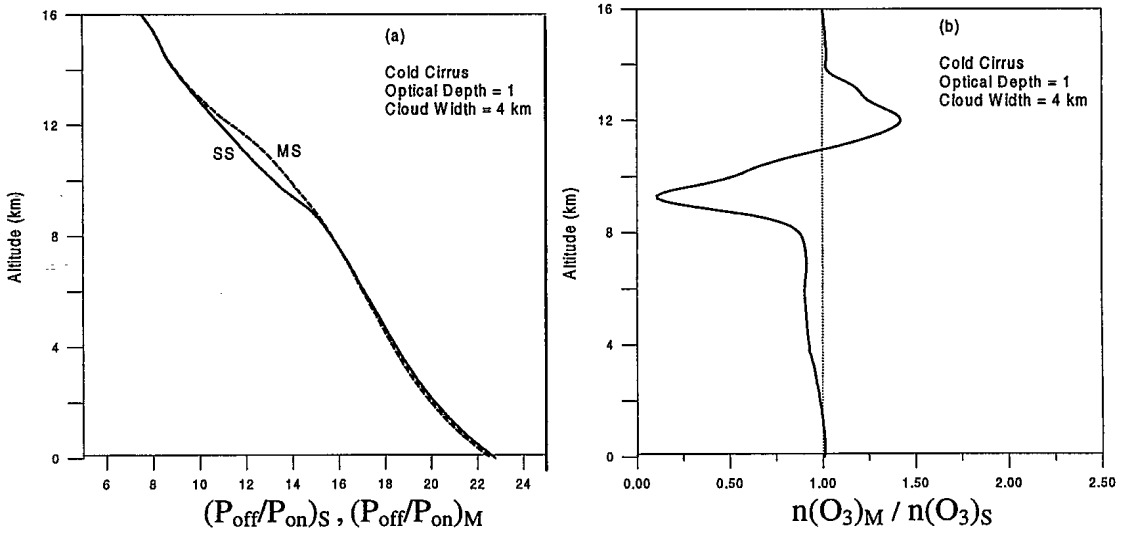

Fig. 9. (a) Ratio of signals for off and on wavelengths for SS (solid curve) and for MS included (dashed curve) in the presence of CC peaked at 12 km with $\Delta z = 4$ km and $\tau = 1$. (b) For the same CC the ratio of retrieved ozone profiles with and without MS.

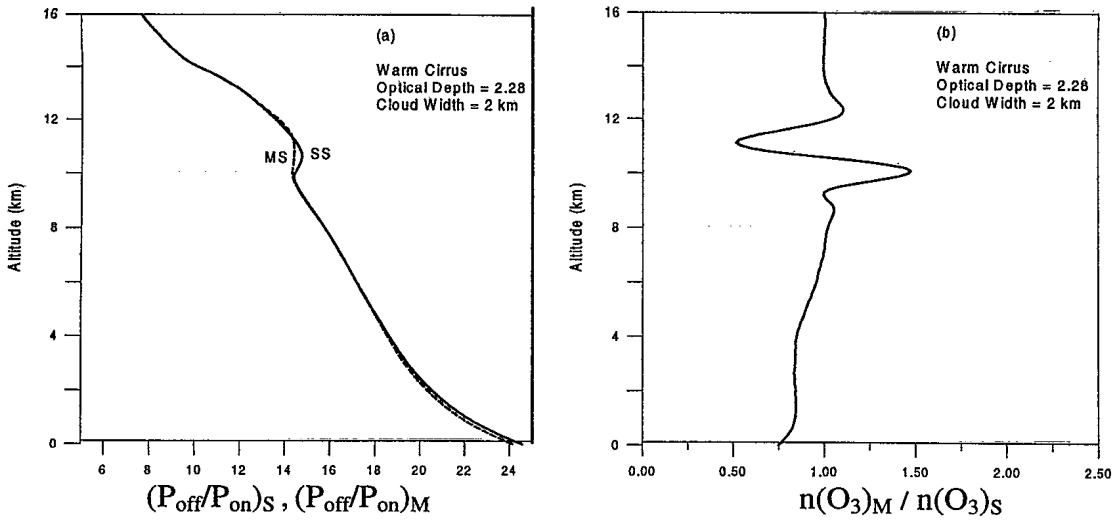

Fig. 10. (a) Ratio of signals for off and on wavelengths for SS (solid curve) and for MS included (dashed curve) in the presence of WC peaked at 12 km with $\Delta z = 2$ km and $\tau = 2.28$. (b) For the same WC the ratio of retrieved ozone profiles with and without MS.

crease in ozone (close to 100%) owing to MS as the pulse penetrates the cloud and then a decrease before the pulse exits the cloud. After the pulse exits the cloud the ozone in the clear air is underestimated by approximately 10%, which recovers by the time the pulse reaches the ground.

The presence of the cirrus causes a discontinuity in the signal ratios, resulting in an excursion in the slope of the signal ratios. This overriding excursion, which recovers as the pulse exits the cloud, relates to the basic nature of ozone retrieval in the DIAL, in which the slope of the ratios of signals is calculated from a sliding window. Therefore the ozone in this range is not reliable. However, it does become reliable from approximately a few kilometers below the cloud base to the ground level.

When the optical depth of CC is kept at 1 but the cloud is spread from $\Delta z = 2$ km to $\Delta z = 4$ km, the ratios $(P_{\text{off}}/P_{\text{on}})_S$, $(P_{\text{off}}/P_{\text{on}})_M$ are as shown in Fig. 9(a). In this case the depression in the ratios within the cloud at SS is smaller, and the buildup in MS continues for a considerable distance below the cloud. It can be mentioned here that the assumed cloud is a Gaussian with its wings extending beyond 2 km (half-width) below the cloud peak. As shown in Fig. 9(b), the net effect of spreading the cloud around its peak and keeping its optical depth constant is that the slope of the ratios of the signals exhibits an excursion smaller than the one in Fig. 8. The effect of MS is to show higher ozone by approximately 45% in the top side of the cloud, then a considerable reduction. The ratio $n(O_3)_M/n(O_3)_S$ seems to recover from the excursion within the cloud at an altitude of approximately 7 km, below which the ozone retrieval is reliable with

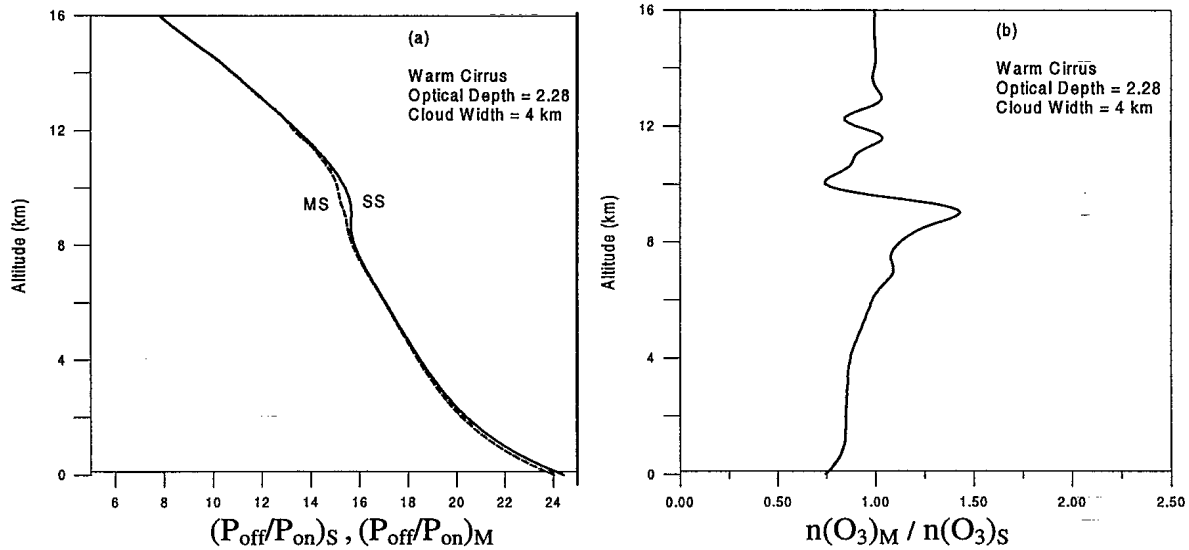

Fig. 11. (a) Ratio of signals for off and on wavelengths for SS (solid curve) and for MS included (dashed curve) in the presence of WC peaked at 12 km with $\Delta z = 4$ km and $\tau = 2.28$. (b) For the same WC the ratio of retrieved ozone profiles with and without MS.

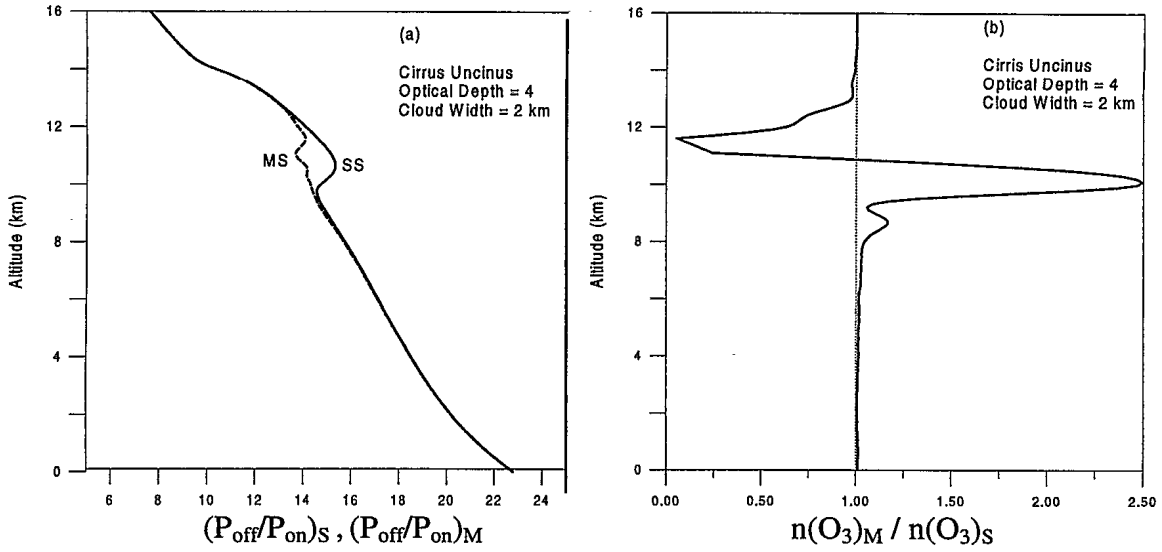

Fig. 12. (a) Ratio of signals for off and on wavelengths for SS (solid curve) and for MS included (dashed curve) in the presence of CU peaked at 12 km with $\Delta z = 2$ km and $\tau = 4$. (b) For the same CU the ratio of retrieved ozone profiles with and without MS.

values being underestimated by approximately 10%. This underestimation also slowly recovers as the pulse continues down and finally results in a slight overestimation in the last kilometer.

A change in cloud type provided a change in effective radius, thus affecting the contribution of differential MS at the two DIAL wavelengths. The effect of a change in cirrus type as well as optical depth is examined in the following. The results of a WC with $\Delta z = 2$ km and an optical depth of $\tau = 2.28$ are shown in Fig. 10. A noticeable difference here is that, not only the $(P_{\text{off}}/P_{\text{on}})_M$ ratio is enhanced owing to the WC as in CC, but even $P_{\text{off}}/P_{\text{on}})_S$ is enhanced for the entire part of the cloud [Fig. 10(a)]. The excursion of the ratio $n(O_3)_M/n(O_3)_S$, as shown in Fig. 10(b), is quite different from that in CC. Below the cloud, however, the MS causes an underestimation of ozone that continues to increase, reaching a ratio of 0.75.

When this WC is spread over $\Delta z = 4$ km, the SS and MS ratios extend to lower altitudes, as shown in Fig. 11(a), with the SS ratio higher than the MS ratio. The corresponding $n(O_3)_M/n(O_3)_S$ ratio goes through multiple excursions, as shown in Fig. 11(b). For WC with $\Delta z = 4$ km the effect of MS on ozone retrieval is an underestimation of ozone in the top side of the cloud and then an underestimation in the bottom side of the cloud, which is quite similar to that for a WC with $\Delta z = 2$ km.

The CC and the WC considered above had effective radii of approximately 12 and 13.3 μm, respectively, with relatively more larger particles included in the WC size distributions. The effective radius of the

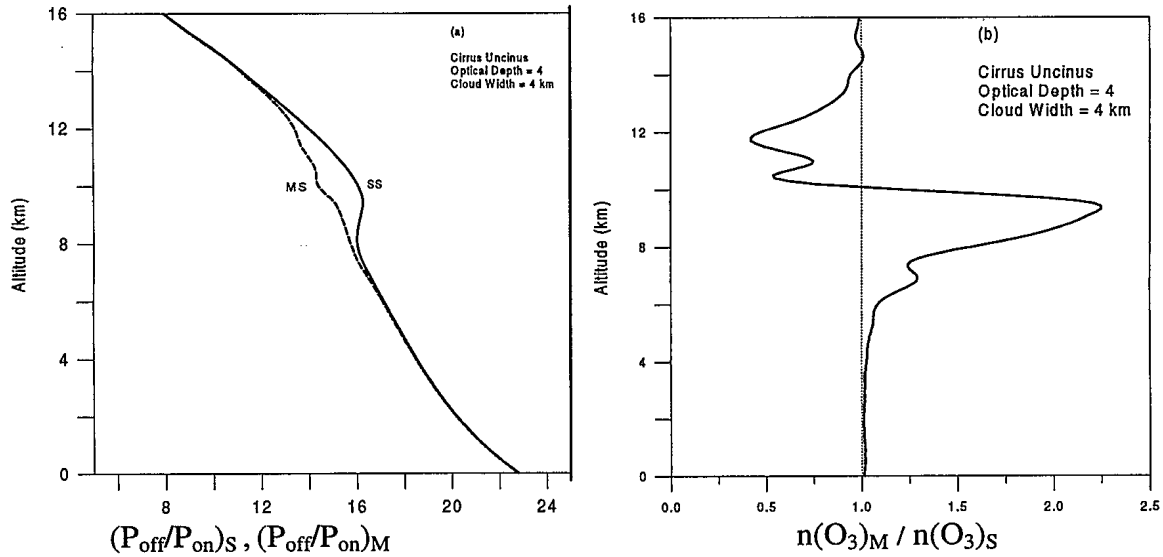

Fig. 13. (a) Ratio of signals for off and on wavelengths for SS (solid curve) and for MS included (dashed curve) in the presence of CU peaked at 12 km with $\Delta z = 4$ km and $\tau = 4$. (b) For the same CU the ratio of retrieved ozone profiles with and without MS.

CU assumed for this study is approximately 24 μm. This significant increase in effective radius is expected to cause a different contribution to MS and therefore to the ozone retrieval through a CU. Figure 12(a) shows the $(P_{off}/P_{on})_S$, $(P_{off}/P_{on})_M$ ratios for a CU with $\Delta z = 2$ km and $\tau = 4$. The curve labeled SS shows much higher values than in previous cases because the scattering at the longer wavelength (315 nm) is relatively higher that at the shorter wavelength (305 nm), although the difference in wavelength is only 10 nm. The high scattering at both wavelengths is also due to the fact that the cirrus is much denser here. This ratio with MS included (labeled MS) does follow the same path as the SS but with considerable divergence between the two under the cloud peak.

The ozone retrieval with and without MS is again exhibited as the ratio $n(O_3)_M/n(O_3)_S$ in Fig. 12(b). The presence of CU causes a high degree of excursion in this ratio, showing a 100% underestimation around the cloud peak and a 150% overestimation below the cloud base, which then starts to settle down at an approximately 8-km altitude.

Below this level highly accurate ozone measurements are possible. It should, however, be pointed out here that the accuracy of ozone measurement is determined on the basis of the strength of the signal-to-noise ratio available from a scattering point, which in the presence of a dense cloud like this CU may be too low. This ratio depends on the system parameters. Therefore, depending on the system, a retrieved ozone value from the range between 8 km and the ground level may not be highly accurate. The curve of Fig. 12(b) indicates only that the effect of MS on ozone retrieval is low in this situation.

When τ of CU is kept the same and the cloud thickness is doubled to 4 km, the signal ratios also spread out as in Fig. 13(a). The corresponding ozone ratio, as shown in Fig. 13(b), remains unreliable during the span of the cloud as well as below the cloud base, extending to an approximately 5-km altitude. Thereafter the effect of MS on ozone retrieval becomes negligible.

4. Conclusion

This study has shown that the effect of MS on space DIAL ozone retrieval is negligible in the main stratospheric ozone layer and in most of the troposphere. The effect of MS starts to become significant in the boundary-layer aerosol. This effect is considerable in the LV conditions, which do occur often in a marine environment. Therefore the ozone measurements in the troposphere made with a space DIAL have to be treated with caution. In situations when elevated aerosol levels occur in the boundary layer as well as in the troposphere the ozone measurements would require MS correction. No effort in this direction appears in the published literature.

The analysis of correction terms T_R, T_β, and T_σ shown in Figs. 5 and 6 suggests that these terms are not important for stratospheric ozone retrieval. However, they are important in the troposphere. Therefore for ozone retrievals in the troposphere with required high accuracies it is highly desirable to retrieve aerosol and Rayleigh information at the DIAL wavelengths. A global ozone measurement is expected to experience high variability in tropospheric conditions. Therefore it would be ideal to derive aerosol extinction and backscatter coefficients in the same DIAL experiment.

In the presence of cirrus clouds, the effect of MS does not permit reliable ozone retrieval within the confines of the cloud itself as well as for some distance below the cloud base. Although the effect of cirrus extends below the cloud base, the retrieval may yield an underestimation or a realistic ozone value depending on the size distribution in the cirrus. The larger size particles tend to favor higher accuracy. In the presence of thin cirrus, however, the boundary-layer ozone values could be acceptable with caution.

The financial support for this study was provided by the Canadian Space Agency, and the research by CRESTech was performed under a subcontract from Optech, Inc., 100 Wildcat Road, North York, Toronto, Canada.

References

1. D. M. Winker, R. H. Couch, and M. P. McCormick, "An overview of LITE: NASA's Lidar in Space Technology Experiment," Proc. IEEE, **14,** 164–180 (1996).
2. A. Ben-David, "Multiple-scattering effects on differential absorption for the transmission of a plane-parallel beam in a homogeneous medium," Appl. Opt. **36,** 1386–1398 (1997).
3. C. Flesia and A. V. Starkov, "Multiple scattering from clear atmosphere observed by transparent crystal clouds in satellite-borne lidar sensing," Appl. Opt. **35,** 2637–2647 (1996).
4. W. Steinbrecht and A. I. Carswell, "Evaluation of the effects of Mount Pinatubo aerosol on differential absorption lidar measurements of stratospheric ozone," J. Geophys. Res. **100,** 1215–1233 (1965).
5. V. A. Kovalev and M. P. Bristow, "Compensational three-wavelength differential absorption lidar technique for reducing the influence of differential scattering on ozone-concentration measurements," Appl. Opt. **35,** 4790–4797 (1996).
6. A. J. Heymsfield, "Cirrus uncinus generating cells and the evolution of cirroform clouds. Part I: Aircraft observations of the growth of the ice phase," J. Atmos. Sci. **32,** 799–808 (1975).
7. A. J. Heymsfield and C. M. R. Platt, "A parameterization of the particle size spectrum of ice clouds in terms of the ambient temperature and ice water content," J. Atmos. Sci. **41,** 846–855 (1984).
8. L. R. Bissonnette, "Multiple-scattering lidar equation," Appl. Opt. **35,** 6449–6465 (1996).
9. I. L. Katsev, E. P. Zege, A. S. Prikhach, and I. N. Polonsky, "Efficient technique to determine backscattered light power for various atmospheric and oceanic sounding and imaging systems," J. Opt. Soc. Am. **A14,** 1338–1346 (1997).
10. F. Nicolas, L. R. Bissonette, and P. H. Flamant, "Lidar effective multiple-scattering coefficients in cirrus clouds," Appl. Opt. **36,** 3458–3468 (1997).
11. D. M. Winker, "Multiple scattering effects observed in LITE data: the good, the bad, and the ugly," in *Proceedings of the Eighth International Workshop on Multiple Scattering Lidar Experiments*, L. Bissonnette, ed. (Defence Research Establishment, Valcartier, Quebec, Canada, 1996), pp. 1–5.

#509382